THE ASTROPHYSICAL JOURNAL, 535:593–601, 2000 June 1

COSMOLOGICAL SMOOTHED PARTICLE HYDRODYNAMIC SIMULATIONS WITH FOUR MILLION PARTICLES: STATISTICAL PROPERTIES OF X-RAY CLUSTERS IN A LOW-DENSITY UNIVERSE

KOHJI YOSHIKAWA
Department of Astronomy, Kyoto University, Kyoto 606-8502, Japan; kohji@kusastro.kyoto-u.ac.jp
AND
Y. P. JING AND YASUSHI SUTO
Department of Physics and Research Center for the Early Universe, School of Science, University of Tokyo, Tokyo 113-0033, Japan; jing@utap.phys.s.u-tokyo.ac.jp, suto@phys.s.u-tokyo.ac.jp
Received 1999 September 14; accepted 2000 January 7

ABSTRACT

We present results from a series of cosmological smoothed particle hydrodynamics (SPH) simulations coupled with the particle-particle-particle-mesh solver for the gravitational force. The simulations are designed to predict the statistical properties of X-ray clusters of galaxies as well as to study the formation of galaxies. We have seven simulation runs with different assumptions about the thermal state of the intracluster gas. Following the recent work by Pearce and coworkers, we modify our SPH algorithm so as to phenomenologically incorporate galaxy formation by decoupling the cooled gas particles from the hot gas particles. All the simulations employ 128^3 particles both for dark matter and for gas components and thus constitute the largest systematic catalogs of clusters simulated in the SPH method performed so far. These enable us to compare the analytical predictions about statistical properties of X-ray clusters against our direct simulation results in an unbiased manner. We find that the luminosities of the simulated clusters are quite sensitive to the thermal history and also to the numerical resolution of the simulations and thus are not reliable. On the other hand, the mass-temperature relation for the simulated clusters is fairly insensitive to the assumptions of the thermal state of the intracluster gas, is robust against the numerical resolution, and in fact agrees well with the analytic prediction. Therefore, prediction of the X-ray temperature functions of clusters on the basis of the Press-Schechter mass function and the virial equilibrium is fairly reliable.

Subject headings: cosmology: miscellaneous — galaxies: clusters: general — methods: numerical

1. INTRODUCTION

Clusters of galaxies have been widely used as probes to extract cosmological information. In particular, cluster abundances including the X-ray temperature function (XTF), X-ray luminosity function (XLF), and number counts turn out to put strong constraints on the cosmological density parameter Ω_0 and the fluctuation amplitude σ_8 (Henry & Arnaud 1991; White, Efstathiou, & Frenk 1993; Jing & Fang 1994; Viana & Liddle 1996; Eke, Cole, & Frenk 1996; Kitayama & Suto 1996, 1997; Kitayama, Sasaki, & Suto 1998). Since the theoretical predictions for those purposes are usually based on the Press-Schechter mass function and the simple virial equilibrium model for the X-ray clusters, the reliability of the resulting constraints is heavily dependent on the validity of those assumptions in the observed X-ray clusters. In fact, there are numerous realistic physical processes that would somehow invalidate the simplifying assumptions employed in the above procedure: one-to-one correspondence between a virialized halo and an X-ray cluster, nonsphericity, substructure and merging, galaxy formation, radiative cooling, heating by the UV background and the supernova energy injection, etc.

While these can be addressed by hydrodynamical simulations in principle, the relevant simulations are quite demanding. This is why most previous studies simply check the Press-Schechter *mass* function against purely N-body simulations in cosmological volume (Suto 1993; Ueda, Itoh, & Suto 1993; Lacey & Cole 1994) or focus on hydrodynamical simulations of individual clusters in a constrained volume (Eke, Navarro, & Frenk 1998; Suginohara & Ostriker 1998; Yoshikawa, Itoh, & Suto 1998); most previous hydrodynamical simulations of clusters in cosmological volume, on the other hand, lacked the numerical resolution to address the above question and/or ignored the effect of radiative cooling (Evrard 1990; Cen & Ostriker 1992, 1994; Kang et al. 1994; Bryan & Norman 1998; Frenk et al. 1999), except for a few of the latest state-of-the-art simulations (Pearce et al. 1999a, 1999b; Cen & Ostriker 1999).

In this paper, we present results from a series of cosmological smoothed particle hydrodynamics (SPH) simulations in cosmological volume with sufficiently high resolution. They enable us to compute the statistical properties of simulated clusters in an unbiased manner and thus to address directly the validity of the widely used model predictions for the mass-temperature relation and the resulting XTFs.

2. SIMULATIONS

Our simulation code is based on the particle-particle-particle-mesh (P^3M)-SPH algorithm, and the P^3M part of the code has been extensively used in our previous N-body simulations (Jing & Fang 1994; Jing & Suto 1998). All the present runs employ $N_{\rm DM} = 128^3$ dark matter particles and the same number of gas particles. We use the spline (S2) softening function for gravitational softening Hockney & Eastwood (1981), and the softening length $\epsilon_{\rm grav}$ is set to $L_{\rm box}/(10N_{\rm DM}^{1/3})$, where $L_{\rm box}$ is the comoving size of the simula-

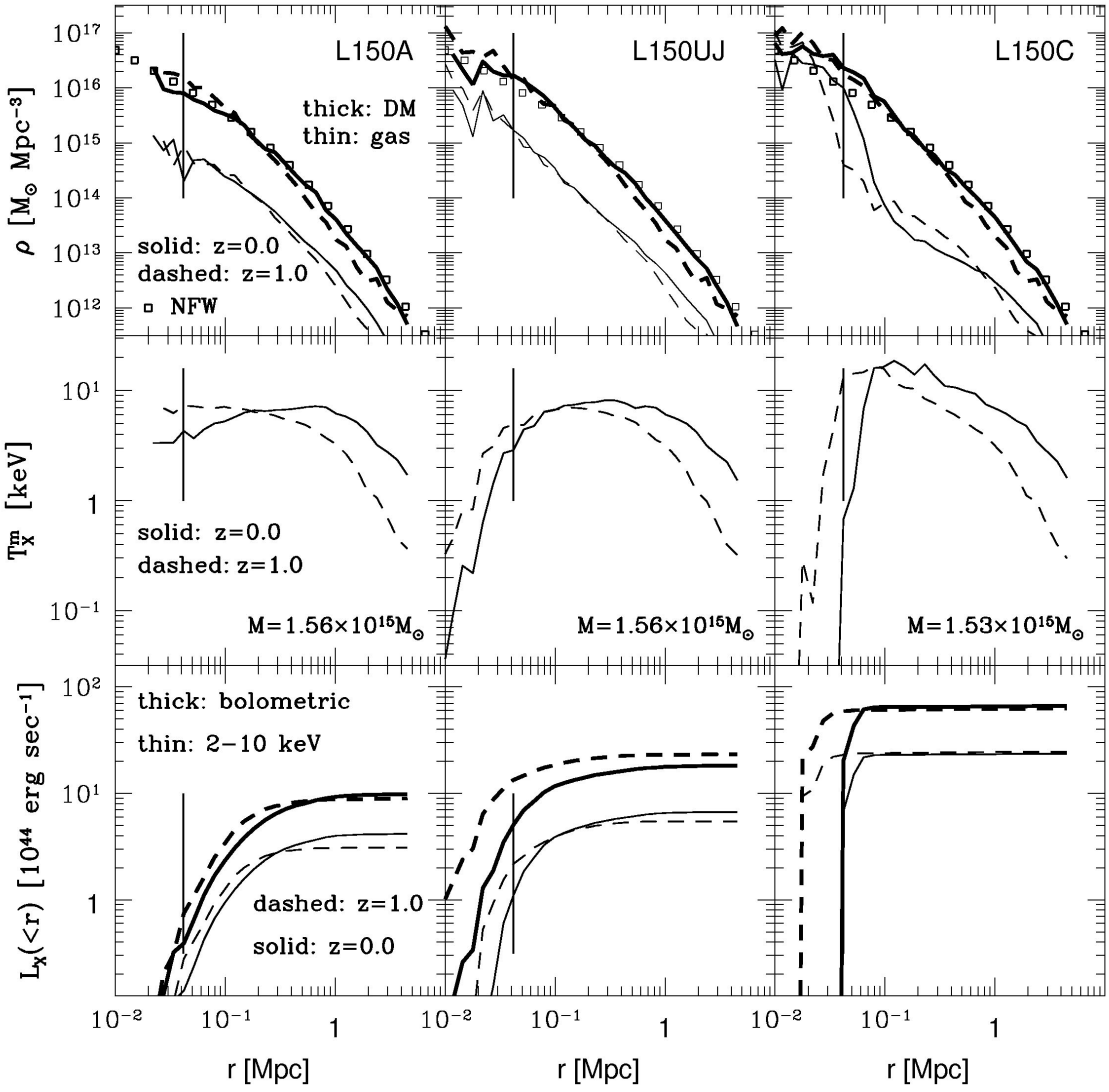

FIG. 1.—Spherically averaged profiles of dark matter and gas densities, ICM temperature, and the integrated X-ray luminosity from the center, for a cluster at $z = 0.0$ (*solid lines*) and $z = 1.0$ (*dashed lines*) in models L150A, L150UJ, and L150C. Vertical lines indicate our lower limit on the SPH smoothing length, $h_{\rm min}$. The virial mass of each cluster at $z = 0.0$ is quoted in the middle panels. For reference, the universal density profile at $z = 0$ (Navarro et al. 1997) corresponding to the virial mass of the cluster is plotted by open squares (*top panels*).

tion box. We set the minimum of SPH smoothing length as $h_{\rm min} = \epsilon_{\rm grav}/4$ and adopt the ideal gas equation of state with an adiabatic index of 5/3.

We consider a spatially flat low-density cold dark matter (CDM) universe with mean mass density parameter $\Omega_0 = 0.3$, cosmological constant $\lambda_0 = 0.7$, and Hubble constant, in units of 100 km s^{-1} Mpc^{-1}, $h = 0.7$. The power-law index of the primordial density fluctuation is set to $n = 1$. We adopt the baryon density parameter $\Omega_b = 0.015\ h^{-2}$ (Copi, Schramm, & Turner 1995) and the rms density fluctuations on a scale of 8 h^{-1} Mpc, with $\sigma_8 = 1.0$, according to the constraints from the *COBE* normalization and cluster abundance (Bunn & White 1997; Kitayama & Suto 1997).

TABLE 1

SUMMARY OF THE SIMULATION MODELS

Model	$L_{\rm box}$ (h^{-1} Mpc)	Cooling	J_{21}^0	$m_{\rm gas}$ ($M_\odot$)[a]	$m_{\rm dark}$ ($M_\odot$)[a]	Cold Gas Decoupling
L150A	150	Off	0.0	2.0×10^{10}	1.7×10^{11}	No
L150C	150	On	0.0	2.0×10^{10}	1.7×10^{11}	No
L150UJ.....	150	On	1.0	2.0×10^{10}	1.7×10^{11}	Yes
L150CJ	150	On	0.0	2.0×10^{10}	1.7×10^{11}	Yes
L75A	75	Off	0.0	2.4×10^{9}	2.2×10^{10}	No
L75C	75	On	0.0	2.4×10^{9}	2.2×10^{10}	No
L75UJ	75	On	1.0	2.4×10^{9}	2.2×10^{10}	Yes

[a] Gas and dark matter mass per particle.

The initial conditions for particle positions and velocities at $z = 25$ are generated using the COSMICS package (Bertschinger 1995). We prepare two different initial conditions for $L_{\rm box} = 150$ and 75 h^{-1} Mpc to examine the effects of the numerical resolution. For the two different box sizes, we consider three cases for the intracluster medium (ICM) thermal evolution (Table 1). L150A and L75A assume nonradiative evolution of the ICM (hereafter nonradiative models). L150C and L75C include the effect of radiative cooling (pure cooling models). In L150UJ and L75UJ (multiphase models), both radiative cooling and UV-background heating are taken into account, and an additional modification of the SPH algorithm is implemented in order to avoid artificial overcooling, following Pearce et al. (1999a, 1999b). In addition, we have L150CJ, which is identical to L150UJ but without the UV background. While the L75C model is evolved until $z = 0.5$, the simulations of the remaining six models are computed up to $z = 0$.

The radiative cooling and the UV-background heating take into account the photoionization of H I, He I, and He II, the collisional ionization of H I, He I, and He II, the recombination of H II, He II, and He III, the dielectronic recombination of He II, Compton cooling, and the thermal bremsstrahlung emission. The UV-background flux density $J(\nu)$ is assumed to be parameterized as

$$J(\nu) = J_{21}(z)\left(\frac{\nu_{\rm L}}{\nu}\right) \times 10^{-21} \ (\text{ergs s}^{-1}\ \text{cm}^{-2}\ \text{sr}^{-1}\ \text{Hz}^{-1}) \ , \tag{1}$$

where $\nu_{\rm L}$ is the Lyman-limit frequency, and we adopt the redshift evolution

$$J_{21}(z) = J_{21}^{0}\,\frac{(1+z)^4}{5+(1+z)^4} \tag{2}$$

following Vedel, Hellsten, & Sommer-Larsen (1994). We use the semi-implicit scheme in integrating the thermal energy equation (Katz, Weinberg, & Hernquist 1996).

It is known that SPH simulations that include the effect of radiative cooling produce unacceptably dense cooled clumps. While Suginohara & Ostriker (1998) ascribed this to some missing physical processes such as heat conduction and heating from supernova explosions, Thacker et al. (1998) and Pearce et al. (1999b) showed that this overcooling could be due to an artificial overestimate of the hot gas density convolved with the nearby cold dense gas particles and can be largely suppressed by simply decoupling the cold gas ($T < 10^4$ K) from the hot component. This numerical treatment can be interpreted as a phenomenological prescription for galaxy formation. Therefore, following their spirit, we adopt a slightly different approach—using the Jeans criterion for the cooled gas:

$$h > \frac{c_s}{\sqrt{\pi G \rho_{\rm gas}}} \ , \tag{3}$$

where h is the smoothing length of gas particles, $\rho_{\rm gas}$ the gas density, c_s the sound speed, and G the gravitational constant. In practice, however, we made sure that the above condition is almost identical to the condition of $T < 10^4$ K adopted by Pearce et al. (1999b). Nevertheless, we prefer using the Jeans criterion because it is rephrased in terms of the physical process. Apart from the fact that such cooled gas particles are ignored when computing the SPH density of hot gas particles, all the other SPH interactions are left unchanged.

3. RESULTS

3.1. *Cluster Identification and Radial Profiles*

At each epoch, we identify gravitationally bound objects using an adaptive "friend-of-friend" algorithm (Suto, Cen, & Ostriker 1992) and select objects with more than 200 dark matter and gas particles as clusters of galaxies. Specifically, we use the SPH gas density in assigning the local linking length with a linking parameter of 0.5. With this parameter, the mass function of the selected clusters is nearly identical to the conventional friend-of-friend with a fixed linking length of 0.2 times the mean particle separation. The virial mass M for each cluster is defined as the total mass at the virial radius within which the averaged mass density is $\simeq 18\pi^2\Omega_0^{0.4}\,\bar{\rho}_c(z)$ predicted from the nonlinear spherical collapse model, where $\bar{\rho}_c(z)$ is the critical density of the universe at z (White et al. 1993; Kitayama & Suto 1996). The X-ray luminosity is computed on the basis of the bolometric and band-limited thermal bremsstrahlung emissivity (Rybicki & Lightman 1979), which ignores metal line emission. We also compute the mass-weighted and emission-weighted temperatures, $T_{\rm X}^m$ and $T_{\rm X}$, using 2–10 keV band emission. For models L150UJ and L75UJ, we do not include the contribution of those cold particles that satisfy criterion (3) in computing $T_{\rm X}$, $T_{\rm X}^m$, and L since they are not supposed to remain as a gaseous component if an appropriate star formation scheme is implemented in our simulation.

In Figure 1, we show the spherically averaged profiles of dark matter and gas densities, ICM temperature, and cumulative X-ray luminosity for the most massive cluster in models L150A, L150UJ, and L150C. Those for models L75A, L75UJ, and L75C are also depicted in Figure 2. The centers of clusters are defined as the peaks of gas density. The profiles of dark matter are fairly well approximated by the model proposed by Navarro, Frenk, & White (1997). Because of an artificial cooling catastrophe, the pure cooling model (L150C and L75C) produces unacceptably high X-ray luminosity, consistent with Suginohara & Ostriker (1998). This artificial feature can be largely removed by decoupling the cold gas from hot component, and models L150UJ and L75UJ yield a fairly reasonable range of X-ray luminosities. Nevertheless, we do not claim that the luminosities in L150UJ and L75UJ are reliable; the current modified scheme is to be interpreted as a tentative and phenomenological remedy at best and should be replaced by a more realistic scheme for galaxy formation. Lewis et al. (1999) have obtained a very similar result based on a more sophisticated treatment of galaxy formation in their simulation. They show that when both cooling and star formation are included in the simulation, cluster luminosities increase only moderately (by a factor of 3) compared to the nonradiative case; this amount of increase is significantly less than that in the pure cooling case. In addition, we find that the values of the luminosities are still significantly affected by the numerical resolution (§ 3.3).

In Figures 3 and 4, we show the spherically averaged profiles of the local dynamical timescale $t_{\rm dyn}$, the two-body heating timescale $t_{\rm 2body}$ (Steinmetz & White 1997), and the cooling timescale $t_{\rm cool}$ for representative clusters with three different mass scales for models L150UJ and L75UJ,

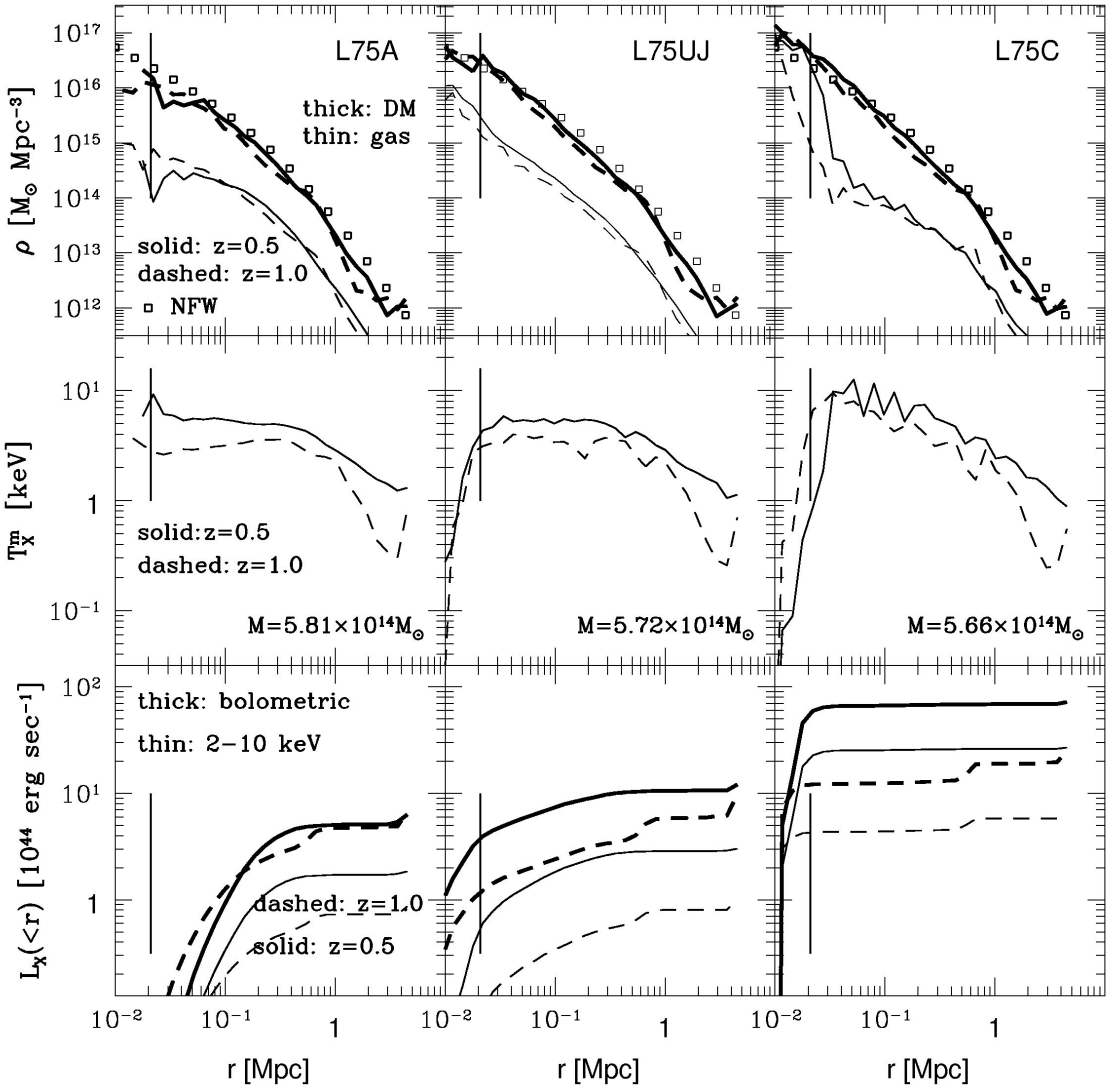

FIG. 2.—Same as Fig. 1 but for models L75A, L75UJ, and L75C at $z = 0.5$ (*solid lines*) and $z = 1.0$ (*dashed lines*). The virial mass of each cluster at $z = 0.5$ is quoted in the middle panels.

respectively. The timescales are defined as

$$t_{\rm dyn} = \frac{1}{\sqrt{G\rho_{\rm tot}}}, \tag{4}$$

$$t_{\rm 2body} = \sqrt{\frac{27}{128\pi}}\,\frac{\sigma_{\rm 1D}^3}{G^2 M_{\rm DM}\,\rho_{\rm DM}\ln\Lambda}, \tag{5}$$

$$t_{\rm cool} = \frac{3n_{\rm gas}\,k_{\rm B}\,T}{2\Lambda_{\rm cool}(n,\,T)}, \tag{6}$$

where G is the gravitational constant, $\rho_{\rm tot}$ the total mass density, $\sigma_{\rm 1D}$ the one-dimensional velocity dispersion of dark matter particles, $\ln\Lambda$ the Coulomb logarithm, $M_{\rm DM}$ the mass of a dark matter particle, $\rho_{\rm DM}$ the mass density of dark matter, $n_{\rm gas}$ the number density of gas, $k_{\rm B}$ the Boltzmann constant, and $\Lambda_{\rm cool}(n, T)$ the cooling function. The expression for $t_{\rm 2body}$ is given in Steinmetz & White (1997), and we set the value of the Coulomb logarithm to $\ln\Lambda = 5$ as a nominal value.

For the clusters with $M \gtrsim 2 \times 10^{14}\ M_\odot$ in the models with $L_{\rm box} = 150\ h^{-1}$ Mpc, $t_{\rm cool}$ is shorter than $t_{\rm 2body}$, and hence artificial two-body heating is not effective for these clusters. On the other hand, clusters with $M \lesssim 10^{14}\ M_\odot$ have the cooling timescale comparable to the two-body heating timescale. Thus, the relatively poor clusters with $M \lesssim 10^{14}\ M_\odot$ in $L_{\rm box} = 150\ h^{-1}$ Mpc models may suffer from the artificial two-body heating. Since it is difficult to predict the possible systematic effect based on the timescale argument alone, it is most straightforward to quantify the effect by a careful comparison with the results in $L_{\rm box} = 75\ h^{-1}$ Mpc runs that are almost free from artificial two-body heating. In the following analysis, we use clusters with $M > 10^{14}$ and $10^{13}\ M_\odot$ for the L150 and L75 models, respectively. Table 2 indicates the number of those clusters that satisfy the above criteria for each model at different redshifts.

It should also be noted that one should not worry about the numerical two-body heating at the central regions of clusters where $t_{\rm dyn} \gg t_{\rm cool}$ even if $t_{\rm cool} \gtrsim t_{\rm 2body}$. As noted in Steinmetz & White (1997), those regions will experience a catastrophic cooling; in fact, they are exactly the place where we attempt to suppress the overcooling by decoupling the cold gas particles.

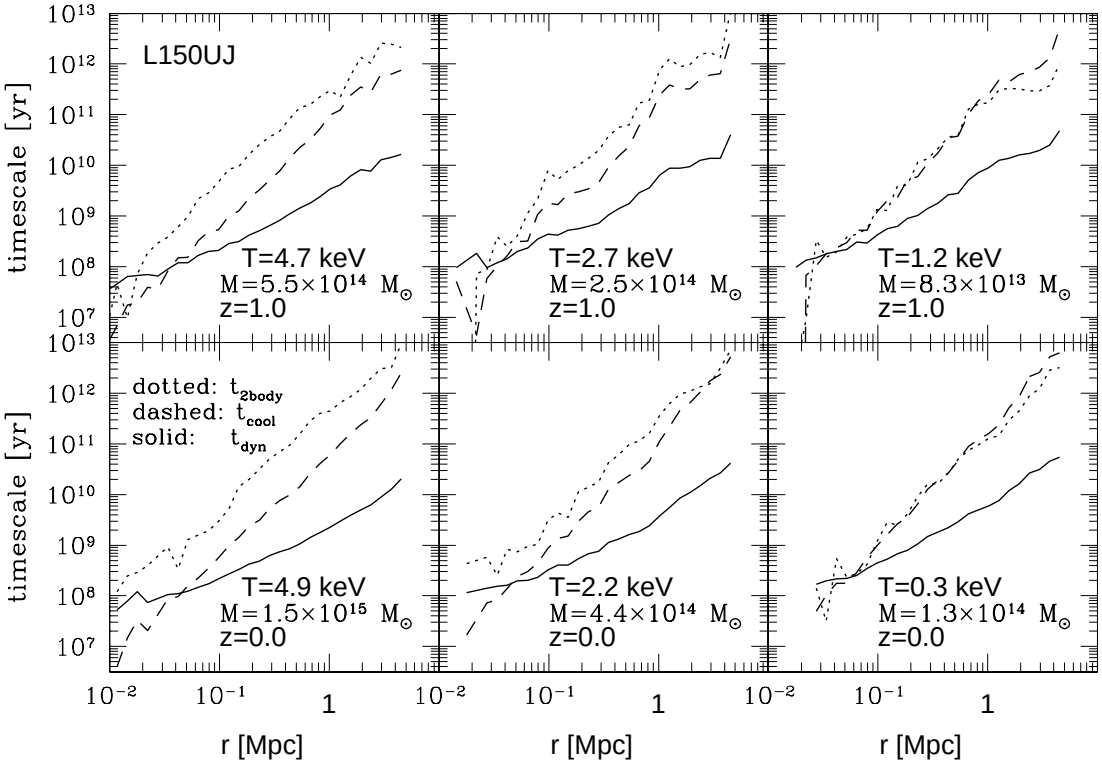

FIG. 3.—Radial profiles of the local dynamical timescale, t_{dyn}, the artificial two-body heating timescale, t_{2body}, and the cooling timescale, t_{cool}, for three different clusters at (*lower panels*) $z = 0.0$ and (*upper panels*) $z = 1.0$ in model L150UJ. The virial mass and temperature are indicated in each panel.

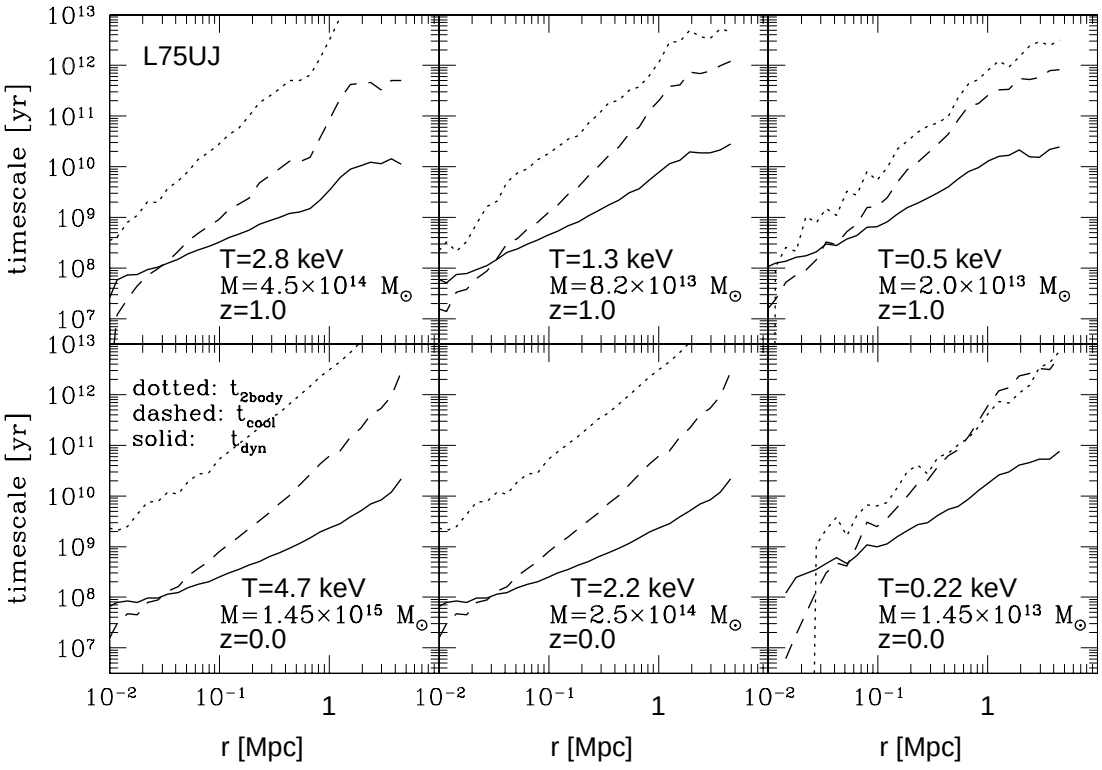

FIG. 4.—Same as Fig. 3 but for model L75UJ

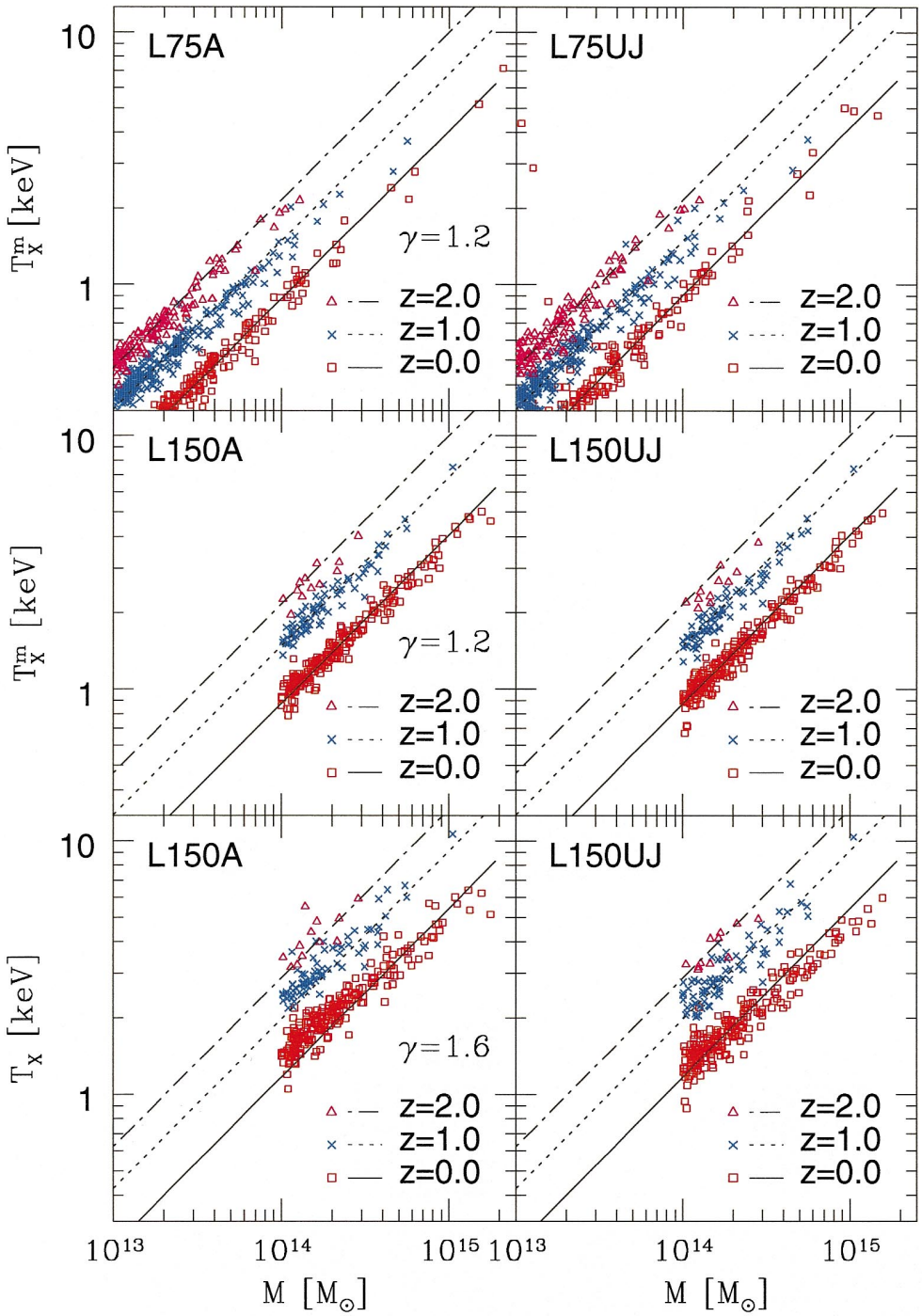

FIG. 5.—Temperature-mass relations for nonradiative and multiphase models at $z = 0.0$, 1.0, and 2.0. The bottom panels show the emission-weighted temperature while others show the mass-weighted temperature. Lines indicate the theoretical model (eq. [7]) with $\gamma = 1.6$ for the emission-weighted temperature and $\gamma = 1.2$ for the mass-weighted one.

3.2. *Temperature-Mass Relation*

A conventional analytical modeling of clusters of galaxies assumes that the ICM is isothermal and in hydrostatic equilibrium within the dark matter potential. Then the ICM temperature is predicted to be

$$k_B T_X = \gamma \frac{\mu m_p GM}{3r_{vir}} \sim 5.2\gamma \left(\frac{\Omega_0 \Delta_c}{18\pi^2}\right)^{1/3} \times \left(\frac{M}{10^{15}\ h^{-1}\ M_\odot}\right)^{2/3} (1 + z_f)\ \text{keV} \qquad (7)$$

TABLE 2

NUMBER OF SIMULATED CLUSTERS THAT WE USED IN THE ANALYSIS

Model	$z = 2.0$	$z = 1.0$	$z = 0.0$
L150A	12	72	224
L150UJ.....	11	76	220
L150C	12	75	222
L75A	123	263	295
L75UJ	117	241	272
L75C	120	245	...

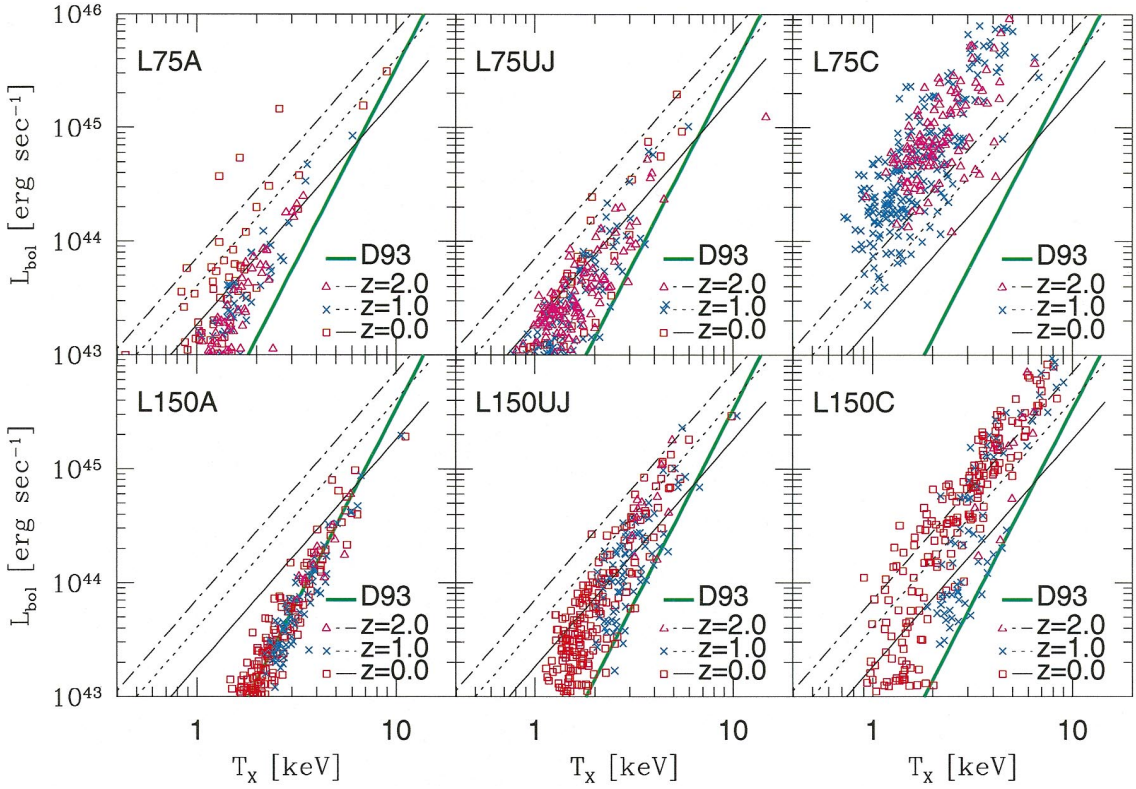

FIG. 6.—Luminosity-temperature relations for nonradiative and multiphase models at $z = 0.0$, 1.0, and 2.0. Relations predicted from self-similar evolution (*light lines*) and the empirical relation from observations (*heavy lines*; David et al. 1993) are shown.

in terms of the cluster mass M, where Δ_c is the mean density of a virialized object at a formation redshift z_f, and γ is a fudge factor of order unity; if the cluster is isothermal and its one-dimensional velocity dispersions are equal to $(GM/3r_{vir})^{1/2}$, then γ is the inverse of the spectroscopic β-parameter and approximately given by 1.2 (Kitayama & Suto 1997).

Since the above T_X-M relation is the most important ingredient in translating the Press-Schechter *mass* function into the XTF, the reliability of the conventional cluster abundance crucially depends on the applicability of this relation. Figure 5 plots the T_X-M relations for nonradiative and multiphase models at $z = 2$, 1, and 0. In order to avoid the possible artificial two-body heating effect, we show the results for clusters of $M > 10^{13}$ and $10^{14}\,M_\odot$ in the L75 and L150 models, respectively.

This figure implies three major conclusions. First, comparison of the upper and middle panels indicates that the current numerical resolution is sufficiently good and that the T_X-M relation seems to be converged. Second, the mass-weighted temperature T_X^m is well fitted to equation (7) with $\gamma = 1.2$, while the emission-weighted temperature T_X is systematically higher for the same M. Finally, the simulated T_X-M relation is almost unaffected by the phenomenological (in the current simulation) treatment of the thermal evolution of the ICM gas, and the results of L150A and L150UJ are almost identical. We also verify that the results of L150CJ are almost identical to those of L150UJ implying that the presence of a UV background does not affect our conclusions. This is the first successful check of the relation, made possible by the sufficiently large volume and good resolution of our simulations.

3.3. *Luminosity-Temperature Relation*

In contrast to the T_X-M relations, the luminosity-temperature relations of X-ray clusters are not easy to predict. This is because the X-ray luminosity is proportional to the square of the gas density and thus sensitive to the thermal evolution of the ICM. A simple self-similar model, which predicts $L_X \propto T_X^2(1 + z_f)^{3/2}$ (Kaiser 1986), is shown to be completely inconsistent with the observed relation of $L_X \propto T_X^\alpha(1 + z)^\zeta$, where $2.6 \lesssim \alpha \lesssim 3.0$ and $\zeta \simeq 0$ (Edge & Stewart 1991; David et al. 1993; Markevitch 1998).

The L_X-T_X relations of our simulated clusters (Fig. 6) also reflect the difficulty in obtaining reliable estimates of the luminosities. While it is reasonable that the results are sensitive to the ICM thermal evolution, they are also affected by the numerical resolution. The cluster luminosities in $L_{box} = 150\ h^{-1}$ Mpc models are systematically underestimated relative to those in $75\ h^{-1}$ Mpc models. Since we employ the equal-mass particle in the simulations, the resolution problem would be more serious for smaller clusters. Actually, this explains why the L150A model produces $L_X \propto T_X^3$ accidentally although this nonradiative model should result in $L_X \propto T_X^2$. Thus, we conclude that the reliable estimation of X-ray luminosities requires much higher resolution than ours, especially for less luminous clusters, in addition to the more physical implementation of the galaxy formation process. Therefore, we disagree with Pearce et al. (1999a), who concluded that the effect of cooling suppresses the X-ray luminosities; while our results do not reach convergence either, we find the opposite trend; i.e., the luminosities increase with the cooling (Figs. 1 and 6). After all, since their resolution is similar to ours, their results cannot

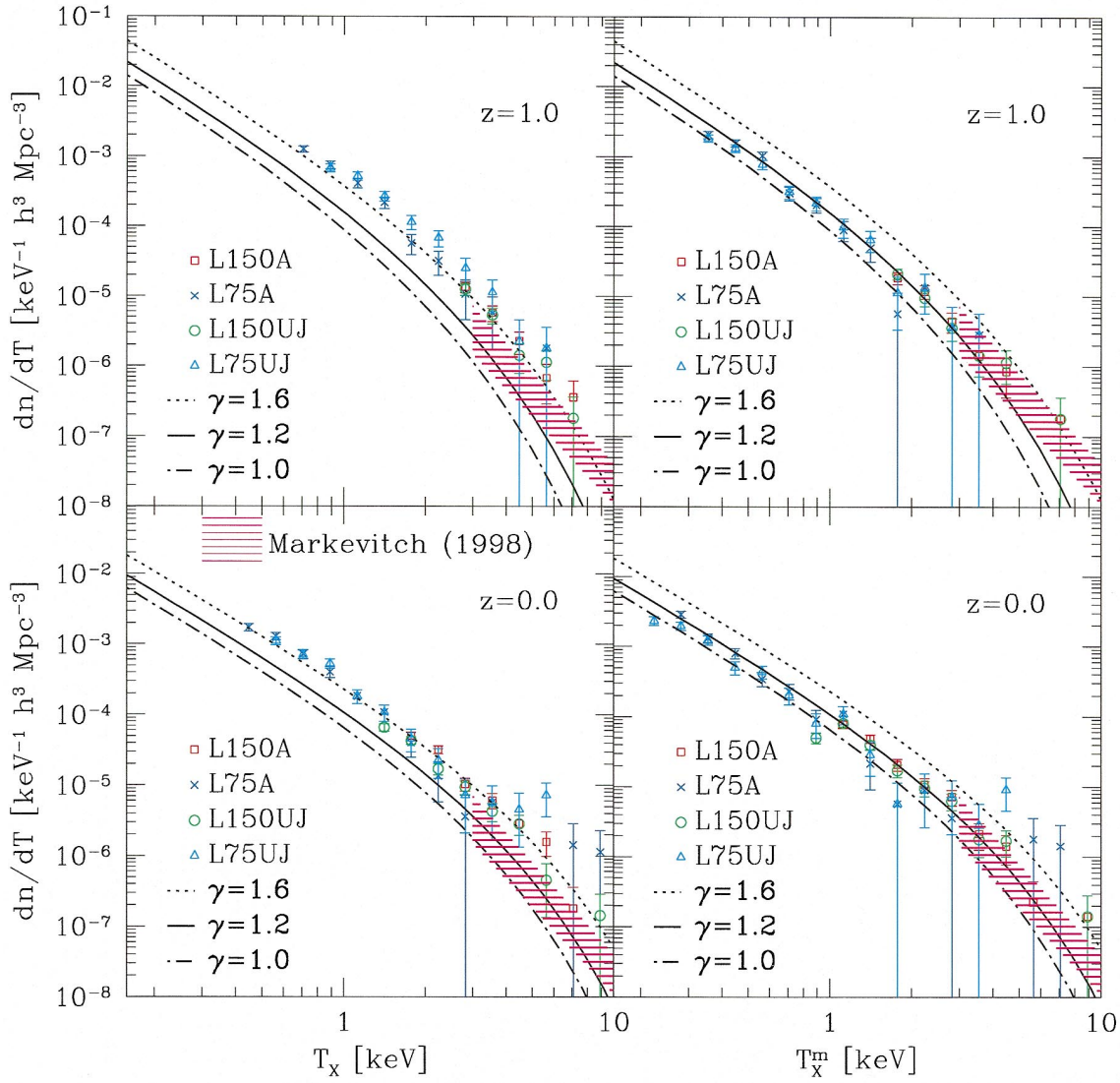

FIG. 7.—X-ray temperature functions at (*bottom*) $z = 0.0$ and (*top*) $z = 1.0$ for each model. The left panels use emission-weighted temperature, whereas the right ones use mass-weighted temperature. Lines are theoretical predictions using the Press-Schechter mass function and T-M relation (eq. [7]) with $\gamma = 1.0$, 1.2, and 1.6. Shaded regions indicate the observed XTF of local ($z < 0.1$) clusters by Markevitch (1998).

escape from the resolution problem, and it is premature to draw any conclusion about the luminosities from cosmological SPH simulations.

3.4. *X-Ray Temperature Function*

Finally, we show the XTFs in nonradiative and multiphase models at redshifts $z = 0.0$ and 1.0 (Fig. 7) as a function of the emission- and mass-weighted temperatures. These should be compared with the analytical prediction on the basis of the Press-Schechter mass function (Press & Schechter 1974) and the T_X-M relation mentioned above. Since we have already showed that the T_X-M relation agrees well with the analytical expectation, our simulated clusters in cosmological volumes can examine the statistical reliability of the analytical prediction of the XTF for the first time. Figure 7 implies that the analytical and numerical results agree well with each other almost independently of the ICM thermal evolution model if we adopt $\gamma \simeq 1.6$ and 1.2 for XTFs in terms of emission- and mass-weighted temperatures, respectively. It should also be noted that, since the XTFs from different numerical resolutions are nearly the same within the statistical errors, we can state that the XTFs from our simulations do not suffer from any serious numerical artifacts. These results justify the use of a simple analytical model for the cluster abundance that has been extensively applied in the past (White et al. 1993; Viana & Liddle 1996; Eke et al. 1996; Kitayama & Suto 1997; Kitayama et al. 1998). The observed XTF of local ($z < 0.1$) clusters by Markevitch (1998) is also shown in Figure 7 and lower by a factor of 2–3 than the simulated ones at $T_X \simeq$ 3–9 keV.

4. CONCLUSIONS

On the basis of a series of large cosmological SPH simulations, we have specifically addressed the reliability of the analytical predictions about the statistical properties of X-ray clusters. In order to distinguish numerical artifacts from real physics, we performed simulations with two different numerical resolutions. Our main findings are summarized as follows.

1. The inclusion of radiative cooling in the high-

resolution simulations substantially changes the luminosities of simulated clusters. Without implementing the galaxy formation scheme, this leads to an artificial overcooling catastrophe, as demonstrated by Suginohara & Ostriker (1998). With a phenomenological prescription of cold gas decoupling like that of Pearce et al. (1999b), however, the overcooling is largely suppressed. Nevertheless, the predicted X-ray luminosities of clusters are not reliable even by 1 order of magnitude.

2. In contrast to the huge uncertainties in the X-ray luminosities, the temperatures of simulated clusters are fairly robust to both the ICM thermal evolution and the numerical resolution and, in fact, are in good agreement with the analytic predictions commonly adopted. We also showed that the emission-weighted temperature is 1.3 times higher than the mass-weighted one.

3. The analytical predictions for the X-ray temperature function translated from the Press-Schechter mass function are fairly accurate and reproduce the simulation results provided that the fudge factor $\gamma = 1.2(1.6)$ is adopted in the mass-weighted (emission-weighted) temperature-mass relation (7). The XTFs simulated in the cosmology adopted in this paper are slightly higher than the observed one for local clusters by Markevitch (1998).

Our simulations have made statistically unbiased synthetic catalogs of clusters of galaxies in virtue of their large simulation volume and sufficient numerical resolution. Thus, they can be the theoretical references that should be compared with the results from future cluster observations with X-ray satellites including *XMM* and *Astro-E* and can contribute to probing cosmological parameters from observed cluster abundances in due course. Additional radiative processes such as heat conduction of the ICM and energy feedback from supernova explosions, which may considerably affect the physical properties of the ICM, must be considered in future works in order to solve the discrepancy in the L-T relation. In addition, since we consider only one fairly specific cosmological model, it is necessary to perform simulations using other cosmological models.

We thank an anonymous referee for pointing out the importance of the two-body heating in the simulations. K. Y. and Y. P. J. gratefully acknowledge the fellowship from the Japan Society for the Promotion of Science. Numerical computations were carried out on VPP300/16R and VX/4R at the Astronomical Data Analysis Center (ADAC) of the National Astronomical Observatory, Japan, as well as at the Research Center for the Early Universe, University of Tokyo (RESCEU) and the High-Energy Accelerator Research Organization, Japan (KEK). This research is supported by Grants-in-Aid by the Ministry of Education, Science, Sports, and Culture of Japan to RESCEU (07CE2002) and by the Supercomputer Project (99-52) of KEK.

REFERENCES

Bertschinger, E. 1995, preprint (astro-ph/9506070)
Bryan, G. L., & Norman, M. L. 1998, ApJ, 495, 80
Bunn, E. F., & White, M. 1997, ApJ, 480, 6
Cen, R., & Ostriker, J. P. 1992, ApJ, 393, 417
———. 1994, ApJ, 429, 4
———. 1999, ApJ, 519, 109
Copi, C. J., Schramm, D. N., & Turner, M. S. 1995, ApJ, 455, 95
David, L. P., Slyz, A., Jones, C., Forman, W., & Vrtilek, S. D. 1993, ApJ, 412, 479
Edge, A. C., & Stewart, G. C. 1991, MNRAS, 252, 428
Eke, V. R., Cole, S., & Frenk, C. S. 1996, MNRAS, 282, 263
Eke, V. R., Navarro, J. F., & Frenk, C. S. 1998, ApJ, 503, 569
Evrard, A. E. 1990, ApJ, 363, 349
Frenk, C. S., et al. 1999, ApJ, 525, 554
Henry, J. P., & Arnaud, K. A. 1991, ApJ, 372, 410
Hockney, R. W., & Eastwood, J. W. 1981, Computer Simulation Using Particles (New York: McGraw Hill)
Jing, Y. P., & Fang, L. Z. 1994, ApJ, 432, 438
Jing, Y. P., & Suto, Y. 1998, ApJ, 494, L5
Kaiser, N. 1986, MNRAS, 222, 323
Kang, H., Cen, R., Ostriker, J. P., & Ryu, D. 1994, ApJ, 428, 1
Katz, N., Weinberg, D. H., & Hernquist, L. 1996, ApJS, 105, 19
Kitayama, T., Sasaki, S., & Suto, Y. 1998, PASJ, 50, 1
Kitayama, T., & Suto, Y. 1996, ApJ, 469, 480
Kitayama, T., & Suto, Y. 1997, ApJ, 490, 557
Lacey, C., & Cole, S. 1994, MNRAS, 271, 676
Lewis, G. F., Babul, A., Katz, N., Quinn, T., Hernquist, L., & Weinberg, D. H. 1999, preprint (astro-ph/9907097)
Markevitch, M. 1998, ApJ, 504, 27
Navarro, J. F., Frenk, C. S., & White, S. D. M. 1997, ApJ, 490, 493
Pearce, F. R., Couchman, H. M. P., Thomas, P. A., & Edge, A. C. 1999a, preprint (astro-ph/9908062)
Pearce, F. R., et al. 1999b, ApJ, 521, L99
Press, W. H., & Schecter, P. 1974, ApJ, 187, 425
Rybicki, G. B., & Lightman, A. P. 1979, Radiative Processes in Astrophysics (New York: Wiley)
Steinmetz, M., & White, S. D. M. 1997, MNRAS, 288, 545
Suginohara, T., & Ostriker, J. P. 1998, ApJ, 507, 16
Suto, Y. 1993, Prog. Theor. Phys., 90, 1173
Suto, Y., Cen, R., & Ostriker, J. P. 1992, ApJ, 395, 1
Thacker, R. J., Tittley, E. R., Pearce, F. R., Couchman, H. M. P., & Thomas, P. A. 1998, preprint (astro-ph/9809221)
Ueda, H., Itoh, M., & Suto, Y. 1993, ApJ, 408, 3
Vedel, H., Hellsten, U., & Sommer-Larsen, J. 1994, MNRAS, 271, 743
Viana, P. T. P., & Liddle, A. R. 1996, MNRAS, 281, 323
White, S. D. M., Efstathiou, G., & Frenk, C. S. 1993, MNRAS, 262, 1023
Yoshikawa, K., Itoh, M., & Suto, Y. 1998, PASJ, 50, 203